AN ABSTRACT OF THE THESIS OF

Haiyan Wang for the degree of Master of Science in Physics presented on February 14, 2000.

Title: Relation between Bandstructure and Magnetocrystalline Anisotropy: Iron and Nickel.

Abstract approved: Redacted for Privacy

Henri J. F. Jansen

A large amount of research has been done in which the magnetocrystalline anisotropy energy for fcc Ni and bcc Fe was calculated based on the electronic structure of these elements. Unfortunately, the results of these studies don't agree with each other and also differ from the experimental observation. In a previous thesis the effects of numerical errors in the Brillouin zone integrations were investigated. The resuls of that work explain why different calculations give different results, but do not explain the difference with experiment. The conclusion was that the underlying bandstructure, which was calculated using standard approximations, was not correct.

The bandstructure of these elements will be different when improved prescriptions for the exchange-correlation energy are used. There is, however, no clear indication along which lines this approximation should be improved. Here we have taken a different approach to change the bandstructure. We suspected that some important interactions between different atomic orbitals are either ignored or miscounted. In this work, we examined the sensitivity of the energy on the interaction between those orbitals and studied in detail the consequences of

changes in some interaction parameters which gave rise to a large energy change. The main result of this work is a better understanding of the relation between changes in the electronic structure in k-space and the resultant change in the magnetocrystalline anisotropy energy. In addition, this work takes another step in trying to find a better understanding how the magnetocrystalline anisotropy energy relates to interactions between neighboring atoms.

Relation between Bandstructure and Magnetocrystalline Anisotropy: Iron and Nickel

by

Haiyan Wang

A Thesis

submitted to

Oregon State University

in partial fulfillment of
the requirements for the
degree of

Master of Science

Completed February 14, 2000
Commencement June 2000

Master of Science thesis of Haiyan Wang presented on February 14, 2000

APPROVED:

Redacted for Privacy

Major Professor, representing Physics

Redacted for Privacy

Chair of the Department of Physics

Redacted for Privacy

Dean of the Graduate School

I understand that my thesis will become part of the permanent collection of Oregon State University libraries. My signature below authorizes release of my thesis to any reader upon request.

Redacted for Privacy

Haiyan Wang, Author

ACKNOWLEDGMENT

I would especially like to express my appreciation to my advisor, Dr. Henri Jansen, for all the time and energy he has spent to guide me to finish this thesis, for all the help he has offered to put this together. I am so lucky to be able to work with such a great professor.

My thanks also go to Guenter Schneider, who set up the basis for my calculation early in his work and spent a lot of time getting me started, his clean coding made it a lot easy for me to pick up.

I am grateful to my officemate David Matusevich, who has been extremely helpful when I ever ran into trouble in the office.

Finally, I would like to thank my husband Yan Zhao for his support.

Financial support was provided by ONR under grant N00014-9410326.

TABLE OF CONTENTS

LIST OF FIGURES

LIST OF FIGURES (Continued)

LIST OF FIGURES (Continued)

Figure Page

LIST OF TABLES

RELATION BETWEEN BANDSTRUCTURE AND MAGNETOCRYSTALLINE ANISOTROPY: IRON AND NICKEL

1. INTRODUCTION

Magnetic materials play an important role in today's technology. An important quantity that has been studied often is the magnetic anisotropy of an ideal system. This quantity determines how the energy of a system varies when the direction of the external magnetic field changes. The most important contribution to the magnetic anisotropy is due to the shape of the sample. This shape anisotropy is a quantity that can be calculated easily. The magnetocrystalline anisotropy is the anisotropy due to the fact that the crystalline arrangement of the atoms is not spherically symmetric. It can be deduced from experiments after the effects of extrinsic properties such as the sample shape have been taken into account.

Magnetocrystalline anisotropy causes the magnetization to orient along a certain prefered direction in the crystal. The prefered direction of magnetization is called the easy axis, and the hard axis of magnetization is the one along which a large magnetic field H_a is required to saturate the magnetization. For bcc crystalline Fe the easy axis is along one of the $\langle 100 \rangle$ crystal directions and the hard axis is along the $\langle 111 \rangle$ direction. For fcc crystaline Ni, the easy and hard axes of magnetization are along the $\langle 111 \rangle$ and $\langle 100 \rangle$ respectively.

The free energy of a spherical crystal per unit volume as a function of the direction of the magnetization can be expanded in terms of the direction cosines α_i. This expansion must be consistent with the crystal symmetry. In a cubic system, we have:

$$E_a = K_0 + K_1 S + K_2 P + K_3 S^2 + K_4 SP + ... \tag{1.1}$$

where

$$S = \alpha_1^2\alpha_2^2 + \alpha_2^2\alpha_3^2 + \alpha_3^2\alpha_1^2 \text{ and } P = \alpha_1^2\alpha_2^2\alpha_3^2 \tag{1.2}$$

The Ks in the expansion are called anisotropy constants. Using only the term proportional to K_1 generally gives a good approximation since higher anisotropy constants vanish quickly. This follows from a perturbation expansion in terms of spin-orbit coupling strength. The magnetocrystalline anisotropy energy is the difference in energy between two states with the magnetization pointing along the easy axis and hard axis, i.e., $\Delta E = E\langle 100\rangle - E\langle 111\rangle$. $\Delta E < 0$ for positive K_1 and $\Delta E > 0$ for negative K_1. Figure 1.1 [1] shows the corresponding one parameter energy surfaces as a function of the direction of the magnetization.

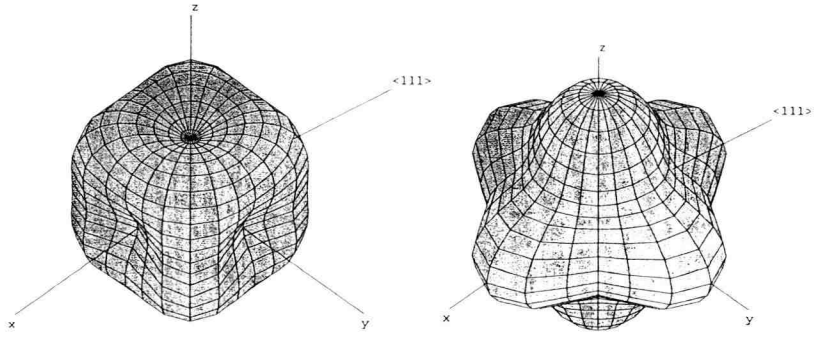

FIGURE 1.1. One parameter cubic anisotropy energy surfaces. The left energy surface is representative for a cubic material like Fe; the energy surface on the right describes a cubic material like Ni.

By the 1930's scientists had realized that magnetocrystalline anisotropy is due to the interplay of the spin moment and the orbital moment caused by spin-

orbit coupling rather than by the pure magneto-static interaction between magnetic dipoles. The results of calculations of the magnetocrystalline anisotropy for the ferromagnetic 3d transition metals remains inconclusive, however, despite the considerable successes of correctly describing many other properties of magnetic systems using density functional theory and the local spin-density approximation. For the cubic materials Fe and Ni the energy difference between the easy and hard axis of magnetization is of order μeV/atom, a value much smaller than typical ground state energies per atom. This magnifies the technical difficulties in calculating the magnetocrystalline anisotropy energy. Many calculations have been carried out, but they do not agree with each other and also differ from the experimental observation even in postdicting the correct easy axis.

For comparative studies, Schneider [1] adopted a tight-binding model to calculate the magnetocrystalline anisotropy energy of *bcc* Fe and *fcc* Ni and studied the numerical precision of the Brillouin zone integrations in great detail. This work is based on the same model to study the dependency of the magnetocrystalline anisotropy on the interaction between atomic orbitals.

2. OVERVIEW OF PREVIOUS CALCULATIONS

In the last ten years many groups have performed calculations of the magnetocrystalline anisotropy energy using different methods and approximations. Compared to the results of calculations prior to 1990 the numerical approximations in these studies are much more consistent, but the results still differ from each other as well as from the experimental value.

Table 1 gives the results of the most recent calculations. In order to improve the convergence of the k-space integration, Daalderop et al. performed semirelativistic linear-muffin-tin-orbital calculations using the linear tetrahedron method plus an adaptive scheme [2]. Guo et al. treated the exchange splitting and the spin-orbit interaction on the same level and performed fully relativistic linear tetrahedron method calculations [3]. Trygg et al. used a full-potential linear-muffin-tin-orbital method that goes beyond a spherical approximation of the potential [4]. Razee used the KKR method and an integration in the complex plane [5]. Halilov used the improved tetrahedron method with only 72-cubed k-points for the Brillouin zone integration which might result in a large uncertainty [6]. Beiden [7] applied a real-space KKR method which avoids the use of k-space integrations, but now is limited in convergence by the number of neighbor shells that can be included in real space, Schneider in his work used the tight-binding model and found the magnetocrystalline anisotropy energy for bcc Fe with the easy axis in agreement with the experiment but wrong easy axis for fcc Ni [1].

The work by Daalderop is very clear in presenting the convergence of the reciprocal space integrations, and his results appear to be well converged. He also estimates the error bars of his numbers, and argues that they are the same as the numbers themselves. None of the other authors (except Schneider) give

			Fe	Ni
Daalderop et al.	(1990)	[2]	-0.5	-0.5
Guo et al.	(1991)	[3]	1.8	-3.1
			–	-2.4
Trygg et al.	(1995)	[4]	-0.5	-0.5
Razee et al.	(1997)	[5]	-0.95	0.11
Halilov et al.	(1998)	[6]	-0.5	0.04
			-2.6	1.0
Beiden et al.	(1998)	[7]	-0.78	-0.43
Schneider	(1999)	[1]	-0.7	-0.15
expt.		[9]	-1.4	2.7

TABLE 2.1. Calculated and experimental magnetic anisotropy energy $\Delta E = E\langle 001\rangle - E\langle 111\rangle$ for bcc Fe and fcc Ni in (μeV/atom).

good indications how well their Brillouin zone integrations are converged. In the paper by Beiden the results of the convergence in real space are presented, and the numbers are in agreement with Daalderop's.

Schneider's results are $\Delta E = -0.7 \pm 0.2\mu$eV/atom for Fe and $\Delta E = -0.15 \pm 0.05\mu$eV/atom for Ni. These results are consistent with Daalderop's, which is remarkable since Schneider's results are based upon a more approximate tight-binding method.

Even though some calculations predict the correct easy axis for Ni, the conclusion based upon the three calculations which present a detailed convergence analysis is that the value for Fe is too small by a factor of two to three and that

the value for Ni is too small by at least a factor of five, and also has the wrong sign. This clearly points at problems in the underlying bandstructure.

All these calculations are based on the local spin density approximation for the exchange-correlation potential. Recent work by Freeman et al. [8] claims that the use of a gradient corrected exchange-correlation potential are in good agreement with experiment. The ultimate goal of our work is to understand how changes in the bandstructure, which could be caused by changes in the exchange-correlation potential, affect changes in the magnetocrystalline anisotropy energy. In this work we took a first step in that direction, and identified the parameters in a tightbinding Hamiltonian which can influence the calculated magnetocrystalline anisotropy energy substantially. The main focus of this work, however, is an investigation of the relation between changes in the electronic structure in k-space and the change in the magnetocrystalline anisotropy energy.

3. THEORY

When atoms are brought together to form solids, the state of valence electrons changes drastically while the state of the inner electrons stays almost the same [10] [11]. Therefore many properties of solids are determined by the valence electrons and only the valence electron states of the atom are considered. The inner electrons are too strongly bound to the atom for significant tunneling to occur to neighboring atoms and they do not give rise to energy bands.

There are huge numbers of atoms and therefore valence electrons in a solid. The motion of those electrons depend on each other, that is each electron's movement is affected by the other electrons. Obviously, it is impossible to find exact solutions for such a multi-electron system. There are several methods to calculate the energy eigenvalues in crystals, each based on some degree of approximation. Examples are the nearly free-electron method, the tight-binding method, the orthogonalized plane waves method, and the pseudo-potential method. The choice of method should be based on the knowledge of the material and the required precision.

The tight binding method is one of the standard methods for solving the periodic potential problem in solids. It is also called the LCAO(Linear Combination of Atomic Orbitals) method. It is an approximation for describing the d bands of the transition metals. It turns out that the tight-binding method correctly describes the symmetry properties of the energy bands. Using the tight-binding method it is relatively easy to get solutions for energy bands at an arbitrary point in the Brillouin zone [12].

The main point of the method is to assume that when an electron is close to an atom it is affected mainly by that atom and the effects due to the other atoms

are much smaller. The tight binding method works very well for large inter-atomic distances (as compared to the radius of the orbit of the valence electrons in the atom) and a strong periodic potential.

First we ignore the effect due to the other atoms, i. e. in the vicinity of each lattice point we assume that the full periodic crystal Hamiltonian H can be approximated by the Hamiltonian of one single atom located at that lattice point. At lattice point $\boldsymbol{R}_m = l_1\boldsymbol{a}_1 + l_2\boldsymbol{a}_2 + l_3\boldsymbol{a}_3$, where $\boldsymbol{a}_i$ are the Bravais lattice basis vectors, the electron moves around $\boldsymbol{R}_m$ in a bound state

$$[-\frac{\hbar^2}{2m}\nabla^2 + V(\boldsymbol{r} - \boldsymbol{R}_m)]\phi_i(\boldsymbol{r} - \boldsymbol{R}_m) = \varepsilon_i\phi_i(\boldsymbol{r} - \boldsymbol{R}_m) \tag{3.1}$$

where ϕ_i is the eigenstate of an electron in an isolated atom, and ε_i is the corresponding eigenvalue. The wave function $\Phi(\boldsymbol{r})$ for an electron in the crystal is determined by

$$[-\frac{\hbar^2}{2m}\nabla^2 + U(\boldsymbol{r})]\Phi(\boldsymbol{r}) = E\Phi(\boldsymbol{r}) \tag{3.2}$$

where $U(\boldsymbol{r})$ is the periodic potential in the crystal which is the sum of $V(\boldsymbol{r} - \boldsymbol{R}_m)$ over all the lattice points, and $\Phi(\boldsymbol{r}) = \sum_m a_m\phi_i(\boldsymbol{r} - \boldsymbol{R}_m)$ is the linear combination of all the atomic orbitals. Here we assume that only one orbital is involved. Inserting $\Phi(\boldsymbol{r})$ into Equation 3.2 and using Equation 3.1, we have

$$\sum_m a_m[\varepsilon_i + U(\boldsymbol{r}) - V(\boldsymbol{r} - \boldsymbol{R}_m)]\phi_i(\boldsymbol{r} - \boldsymbol{R}_m) = E\sum_m a_m\phi_i(\boldsymbol{r} - \boldsymbol{R}_m) \tag{3.3}$$

When the distance between two atoms is larger than the radius of the atom, the overlap between ϕ_i from different lattice points is very small, i. e.

$$\int \phi_i^*(\boldsymbol{r} - \boldsymbol{R}_m)\phi_i(\boldsymbol{r} - \boldsymbol{R}_n)d\boldsymbol{r} = \delta_{nm} \tag{3.4}$$

We multiply $\phi_i^*(\boldsymbol{r}-\boldsymbol{R}_n)$ from the left on both sides of Equation 3.3 and integrate

$$\sum_m a_m\{\varepsilon_i\delta_{mn}+\int\phi_i^*(\boldsymbol{r}-\boldsymbol{R}_n)[U(\boldsymbol{r})-V(\boldsymbol{r}-\boldsymbol{R}_m)]\phi_i(\boldsymbol{r}-\boldsymbol{R}_m)d\boldsymbol{r}\}=Ea_n \quad (3.5)$$

and we finally get

$$\sum_m a_m\int\phi_i^*(\boldsymbol{r}-\boldsymbol{R}_n)[U(\boldsymbol{r})-V(\boldsymbol{r}-\boldsymbol{R}_m)]\phi_i(\boldsymbol{r}-\boldsymbol{R}_m)d\boldsymbol{r}=(E-\varepsilon_i)a_n \quad (3.6)$$

Since $U(\boldsymbol{r})$ is periodic the integral in Equation 3.6 depends only on the relative position $(\boldsymbol{R}_n-\boldsymbol{R}_m)$. The above equation is the secular equation for the crystal which has N primitive cells. According to Bloch's theorem, the eigenstate is

$$\Phi_k(\boldsymbol{r})=\frac{1}{\sqrt{N}}\sum_m e^{-i\boldsymbol{k}\cdot\boldsymbol{R}_m}\phi_i(\boldsymbol{r}-\boldsymbol{R}_m) \quad (3.7)$$

which gives $a_m=\frac{1}{\sqrt{N}}e^{-i\boldsymbol{k}\cdot\boldsymbol{R}_m}$. Therefore the corresponding eigenvalue is

$$E(\boldsymbol{k})=\varepsilon_i+\sum_d J(\boldsymbol{R}_d)e^{-i\boldsymbol{k}\cdot\boldsymbol{R}_d} \quad (3.8)$$

where $J(\boldsymbol{R}_d)$ is the hopping integral

$$J(\boldsymbol{R})=\frac{1}{N}\int\phi_i^*(\boldsymbol{r}-\boldsymbol{R})[U(\boldsymbol{r})-V(\boldsymbol{r})]\phi_i(\boldsymbol{r})d\boldsymbol{r} \quad (3.9)$$

According to Equation 3.8, each $\boldsymbol{k}$ corresponds to one eigenvalue. There are altogether N different values of the crystal momentum, $\boldsymbol{k}$ and hence $E(\boldsymbol{k})$ will form a continuous band when N goes to infinity. It means that when atoms form a solid, atomic states of those atoms will form energy bands in the crystal.

In case more than one atomic orbital is involved, the elements of J in equation 3.8 become matrices and the band energies are found by diagonalizing the Hamiltonian matrix H:

$$J_{i,\sigma;j,\sigma'}(\boldsymbol{R})=\delta_{\sigma,\sigma'}\frac{1}{N}\int\phi_{i,\sigma}^*(\boldsymbol{r}-\boldsymbol{R})[U(\boldsymbol{r})-V(\boldsymbol{r})]\phi_{j,\sigma}(\boldsymbol{r})d\boldsymbol{r} \quad (3.10)$$

$$H_{i,\sigma;j,\sigma'}(\boldsymbol{k}) = \varepsilon_{i,\sigma}\delta_{\sigma,\sigma'}\delta_{i,j} + \sum_{d} J_{i,\sigma;j,\sigma'}(\boldsymbol{R}_d)e^{-i\boldsymbol{k}\cdot\boldsymbol{R}_d} \tag{3.11}$$

The number of energy values for each $\boldsymbol{k}$ is equal to the sum of the number of atomic orbitals on all atoms in the unit cell. If we also include spin in the description the number of atomic orbitals becomes twice as large. Spin-orbit coupling is easily introduced in this case, see Schneider [1]. The Hamiltonian now contains elements that connect the different spin states through the raising and lowering operators in

$$\lambda_{SO} < \sigma|\boldsymbol{S}|\sigma' > \cdot < i|\boldsymbol{L}|j > \tag{3.12}$$

In this work, a parameterized band-structure including s, p and d wave functions is used for *bcc* Fe and *fcc* Ni based on an orthogonal 3 center Slater-Koster tight binding formalism [13] [14]. In our calculation, we just consider the hopping effect up to the second nearest neighbor for *fcc* Ni and third nearest neighbor for *bcc* Fe.

4. BRILLOUIN ZONE INTEGRATION

It is often much more convenient to do the calculation in the reciprocal space. This is the space formed by the vectors $\boldsymbol{k}$ defined in the previous chapter. Reciprocal space is a space defined by a set of vectors – reciprocal vectors. If in real space the primitive lattice vectors are $(\boldsymbol{a}_1, \boldsymbol{a}_2, \boldsymbol{a}_3)$, the primitive reciprocal vectors are defined as:

$$\begin{aligned} \boldsymbol{b}_1 &= 2\pi \frac{\boldsymbol{a}_2 \times \boldsymbol{a}_3}{\boldsymbol{a}_1 \cdot (\boldsymbol{a}_2 \times \boldsymbol{a}_3)} \\ \boldsymbol{b}_2 &= 2\pi \frac{\boldsymbol{a}_3 \times \boldsymbol{a}_1}{\boldsymbol{a}_1 \cdot (\boldsymbol{a}_2 \times \boldsymbol{a}_3)} \\ \boldsymbol{b}_3 &= 2\pi \frac{\boldsymbol{a}_1 \times \boldsymbol{a}_2}{\boldsymbol{a}_1 \cdot (\boldsymbol{a}_2 \times \boldsymbol{a}_3)} \end{aligned} \tag{4.1}$$

The lattice vector and the reciprocal vector has the relationship $\boldsymbol{b}_i \cdot \boldsymbol{a}_j = 2\pi\delta_{ij}$, and $\boldsymbol{k}$ is represented in the reciprocal space as $\boldsymbol{k} = k_1\boldsymbol{b}_1 + k_2\boldsymbol{b}_2 + k_3\boldsymbol{b}_3$. Notice that reciprocal space is also periodic.

In a crystalline solid, physical quantities are evaluated in k-space by

$$\langle X \rangle = \frac{1}{\Omega} \sum_n \int_\Omega d\boldsymbol{k} X_n(\boldsymbol{k}) f(\varepsilon_n(\boldsymbol{k})) \tag{4.2}$$

for some matrix element $X_n(\boldsymbol{k}) = \langle \Phi(\boldsymbol{k}) | X | \Phi(\boldsymbol{k}) \rangle$ and $f(\varepsilon)$ are occupation numbers. At absolute zero, $f = 1$ when $\varepsilon < \varepsilon_F$ and $f = 0$ when $\varepsilon > \varepsilon_F$. Equation 4.2 is integrated over the first Brillouin zone and summed over all bands.

Often, it is either impossible or too expensive to do the integral in Equation 4.2 over all the $\boldsymbol{k}$ points directly, we must seek the aid of approximation in order to achieve the required precision with the minimum number of k-points. Schneider [1] has investigated this in detail. Here we will use the Gaussian broadening method.

By introducing an artificial Fermi surface smearing over a suitably chosen energy range around the Fermi energy level, the rate of convergence of the numerical integrals can be easily improved. Using the Fermi distribution function at a finite temperature is one commonly used smoothing function for Fermi surface smearing. Using the integral over a Gaussian, which arises from a Gaussian broadening of the density of states, is another choice of smoothing function. The weight for each $\boldsymbol{k}$ point becomes

$$\omega_{n,\boldsymbol{k}}(\varepsilon,\mu,T) = \frac{1}{e^{(\frac{\mu-\varepsilon_{n,\boldsymbol{k}}}{k_B T})}+1} \tag{4.3}$$

for the Fermi distribution at a finite temperature and

$$\omega_{n,\boldsymbol{k}}(\mu,\sigma) = \frac{1}{\sigma\sqrt{2\pi}}\int_{-\infty}^{\mu} e^{\frac{-(\epsilon-\varepsilon_{n\boldsymbol{k}})^2}{2\sigma^2}} d\epsilon = \frac{1}{2} erfc(\frac{\varepsilon_n(\boldsymbol{k})-\mu}{\sqrt{2}\sigma}) \tag{4.4}$$

for Gaussian Fermi surface smearing.

Gaussian Fermi surface smearing is chosen in this work, since this is the method of choice in most other calcultations. From a numerical point of view there is no difference between two different smoothing functions. Once we introduce a smoothing function, the calculation of the Brillouin zone integrals is trivial. Since the integrands are periodic functions and we integrate over the full zone, the best way to do the integrals is to use summations over equally spaced points (i.e. a compound trapezoidal rule). Hence we calculate the total energy according to

$$E_{tot} = \frac{1}{N_1 N_2 N_3}\sum_n \sum_{\boldsymbol{k}} E_n(\boldsymbol{k})\omega_{n,\boldsymbol{k}}(\mu,\sigma) \tag{4.5}$$

with the variable μ calculated from the normalization condition

$$N_{tot} = \frac{1}{N_1 N_2 N_3} \sum_n \sum_{\boldsymbol{k}} \omega_{n,\boldsymbol{k}}(\mu, \sigma) \tag{4.6}$$

and where the points in the Brillouin zone are given by

$$\boldsymbol{k} = \frac{1}{N_1 N_2 N_3}(n_1 \boldsymbol{b}_1 + n_2 \boldsymbol{b}_2 + n_3 \boldsymbol{b}_3) \tag{4.7}$$

Although the value of the integral to be calculated is modified by the introduction of a smooth occupation number function many calculated properties are insensitive to the choice of the width σ in Equation 4.4 if this width is chosen sufficiently small. On the other hand, if the width σ is larger, the k-space integral converges more rapidly. The optimal size of k-point mesh to be used depends on the details of the band-structure and also the density of states at the Fermi level affects the choice of σ. Since major contributions to the magnetocrystalline anisotropy energy come from states close to the Fermi level, σ should be at the order of the size of the spin-orbit coupling. Schneider [1] shows in his calculation that for $\sigma >> \lambda_{SO}$, the magnetocrystalline anisotropy energy is proportional to σ^2 and extrapolates to a wrong value. Using a small enough width for Fermi surface smearing parameter will pick up contributions close to the Fermi level correctly and the value for the magnetocrystalline anisotropy energy converges to the same results as obtained by other methods of Brillouin zone integration. For a smaller width σ we must use larger number of k-points, however, in order to get convergence of the magnetocrystalline anisotropy energy. In our calculations we used $N_1 = N_2 = N_3 = 60$ and a value of $\sigma = 49meV$. This is the smallest value of σ for which the number of k-points is still large enough to give converged values of the Brillouin zone integral [1]. The value of σ is larger than needed for a good convergence of the magnetocrystalline anisotropy energy, but the values are close

enough that the changes in the magnetocrystalline anisotropy energy calculated in this study are representative for the changes in the well converged calculations. Limitations in time and space prevented us from making the k-mesh much larger as needed for fully converged calculations.

5. PROCEDURE

We have mentioned before that the most reliable of the currently available calculations for the magnetocrystalline anisotropy energy differ from the experimental observations. We suspected that some important interactions between different atomic orbitals are ignored or miscounted. So we deliberately modified the different matrix elements which describe the intensity of the interaction between different atomic orbitals by small amounts and observed the resultant changes in the magnetocrystalline anisotropy energy in each case. We were hoping to find some large changes in this energy, which would denote a strong sensitivity to a specific interaction. We modified each matrix element, with a change in a range from -0.04 to 0.04 and a step of 0.002. We did this for both spin up and spin down for each matrix element for both Ni and Fe.

To our surprise, we found only a few matrix elements that caused larger changes in the calculated energy. Form this group we chose three cases for both Fe and Ni. These are labeled xyd2_111-up, xyd2_111-down, and xyxy_200-up for Fe and xyd2_110-down, xyxy_011-down, and xyxy_110-down for Ni. The orbitals involved are either xy or d2 from two atoms whose relative position is described by the 3-digits number of the matrix element index, for example, xyd2_111 denotes the interaction of the first nearest neighbour along $\langle 111 \rangle$ direction.

After picking out these matrix-elements that cause larger changes in the calculated energy, we investigated the effects of changes in the parameters with a smaller step size of 0.0002 but still within the same range as before.

In all cases studied we did not see any difference in the bandstructure of the material. All bands were exactly the same in the plots (which are drawn on a scale of several eV), and therefore we needed to look at different ways to analyze

the results. We had expected to see some differences, which could then be related to the changes in the magnetocrystalline anisotropy energy. We first studied the contribution of each band to the total magnetocrystalline anisotropy energy. The idea is that bands near the Fermi energy are the most important.

In the next phase we studied the contributions of the different parts in reciprocal space to the energy changes. In order to do so we make use of the concept of stars. A star $\boldsymbol{k}^*$ of the vector $\boldsymbol{k}$ is the set of all vectors $\boldsymbol{k}$ that are obtained from the original vector by all possible rotations in the cubic group. The reason for using the idea of a star is related to symmetry. In a cubic system without spin-orbit coupling all reciprocal lattice vectors which are elements of the same star have the same set of eigenvalues. If we include spin-orbit coupling, the cubic symmetry is broken, and for an arbitrary direction of the spin moment only the vectors $\boldsymbol{k}$ and $-\boldsymbol{k}$ have the same energy (unless an external magnetic field is present). The changes in the eigenvalues at different elements of a star are, however, related by symmetry. If we calculate the contribution of one vector $\boldsymbol{k}$ to the magnetocrystalline anisotropy energy we find a number on the order of the spin-orbit coupling parameter. If we sum over all elements of a star all these contributions cancel and for a cubic material only terms proportional to the fourth power of the spin orbit coupling strength remain. Therefore, it is important to study the contribution to the energy in terms of stars, in order to eliminate the effects of symmetry from the discussion.

In the next steps we looked at correlations between the contributions of stars and the changes in the magnetocrystalline anisotropy energy. First, we considered the effects of the Fermi energy. Since each time a parameter is changed the Fermi energy is changed, the shape of the Fermi surface will change correspondingly. Some stars may be "pulled" closer to the Fermi surface while some other stars will be "pushed" away from the Fermi surface. We expect especially large contributions

from stars that move through the Fermi surface. Of course, we always have to keep in mind that it is actually the Fermi surface that is changing, not the reciprocal lattice vectors. In order to obtain a measure of the effects of changes in the Fermi surface we studied the correlation between the contribution of a star to the change in magnetocrystalline anisotropy energy and the minimum distance of the energy eigenvalues in the star to the Fermi energy, calculated in the reference state with the original values of the parameters.

The previous calculations gave a huge amount of data. In order to get a better understanding of this data we defined a correlation index for each wave vector in the following manner. We calculate the change in magnetocrystalline anisotropy energy $\Delta MAE(\Delta p)$ as a function of the changes Δp in a specific hopping integral. We also have the contribution $\Delta E(\boldsymbol{k}^*, \Delta p)$ from each star. The correlation index for this star is now defined as

$$C(\boldsymbol{k}^*) = \frac{1}{Norm(E)Norm(\Delta MAE)} \int d\Delta p E(\boldsymbol{k}^*, \Delta p)\Delta MAE(\Delta p) \tag{5.1}$$

where

$$Norm(\Delta MAE) = \left(\int d\Delta p (\Delta MAE(\Delta p))^2 \right)^{\frac{1}{2}} \tag{5.2}$$

and similarly for the normalization of E.

Since the data set is extremely large, we looked at a few selected values of the parameter changes only. We chose the points which give an extreme value on the graph of the overall contribution to the changes in the magnetocrystalline anisotropy energy, the points where the curve crosses the zero line, and sometimes, the points that are half way between zero and the extreme values as the base for

comparison. At each chosen point, we sampled two neighboring points as well. This we did to make sure that we did not see any sudden changes in contributions for small changes in the parameter values. This was never the case, indeed.

For both Fe and Ni we obtained a histogram of the distribution of the stars in terms of the correlation index. Next, we looked at the effects of changes in all six parameters mentioned before and selected the stars whose contributions to the change in energy are either correlated or anti-correlated with the total change. After locating the position of each selected group in the first Brillouin zone, we picked one element from the star and plotted these elements in a three-dimensional box.

Finally, we looked at the relationship between the correlation index and the normalization of the contribution to the star to the total change in energy, which is an indication of the absolute contribution to the change in magnetocrystalline anisotropy energy of that star.

6. RESULT AND DISCUSSION

6.1. Selection of sensitive parameters

When we first modified the matrix elements our intuition was that, since the contribution of the energy due to the hopping effects between two different neighboring atoms is small compare to that due to the "on-site" interaction, the magnetocrystalline anisotropy energy should be most sensitive to changes in the values of the matrix elements. To our surprise, within the range given before, we found out that the largest changes almost all come from the first nearest neighbor elements in Ni. In Fe, we did not see any significant change in energy by modifying the on-site matrix element either. The change in the magnetocrystalline anisotropy energy due to the change in the elements for neighboring atoms could be as high as a factor of 100 compared to the unmodified value. We thus did further study on those elements.

The changes in magnetocrystalline anisotropy energy as a function of parameter change in all six cases used for the following more detailed analysis are given in Figure 6.1.

6.2. Effects of bands near the Fermi energy

We assumed that the largest contributions to the changes in energy should come from the bands that cross the Fermi surface. This was indeed observed. What we did not foresee was that the contribution of each band is actually huge compared to the final change in energy, but that the contributions of different bands tend to cancel each other in great detail. Here we only present the results for the case of parameter xyd2_110, spin down, in Ni. The other five cases are

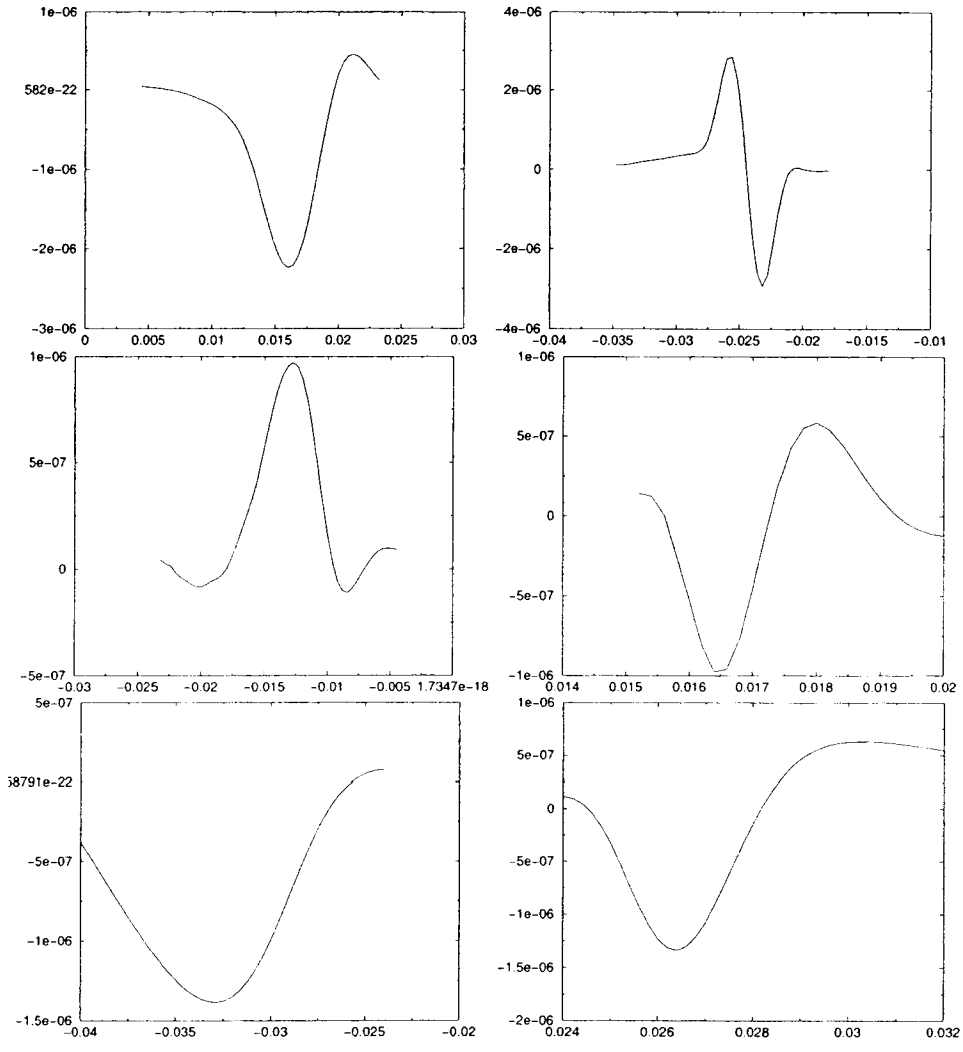

FIGURE 6.1. The change in magnetocrystalline anisotropy energy as a function of parameter change for the selected matrix elements. The left column is for Fe, the right is for Ni. From the top to the bottom, the matrix element being changed for Fe are xyd2_111-up, xyd2_111-down and xyxy_200-up, for Ni, they are xyd2_110-down, xyxy_011-down and xyxy_110-down respectively.

similar. In Ni the bands that cross the Fermi energy are labeled 5 through 12. The lowest four bands are completely occupied. The largest contributions come

from the highest bands. In the following figures, 6.2 to 6.6, we can see how each time when we add several adjacent bands together, the contribution to the energy change is reduced dramatically.

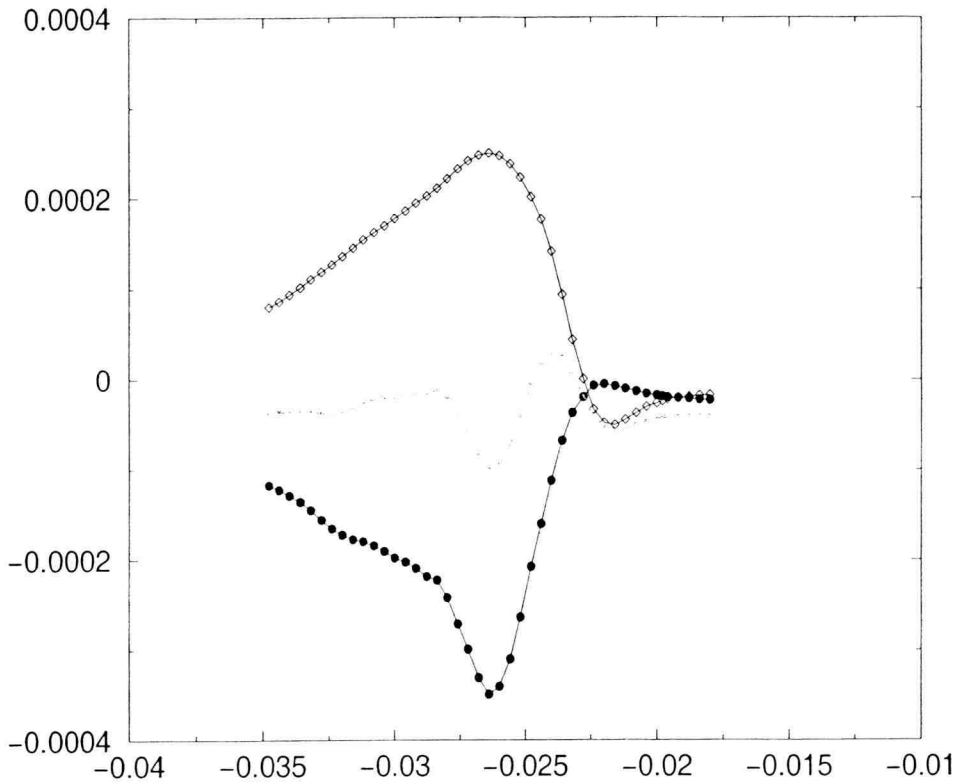

FIGURE 6.2. Change in ΔE for fcc Ni($\lambda_{so} = 100meV$) as a function of one parameter change using Gaussian Fermi surface smearing with $\sigma = 49meV$ and division 60 along a reciprocal lattice vector. The parameter being changed is xyd2_110 spin down. Energy is measured in Rydbergs. The diamond is the contribution from band 12, the filled circle represents the contribution from band 11, and the stars describe the sum of those two bands for each parameter change which will be used in the next step. Bands higher than 12 are not counted because they are above the Fermi energy and unoccupied, thus don't have any contribution

It is interesting to look at the magnitude of the change of magnetocrystalline anisotropy energy in each graph. Every time, the contribution to ΔE is reduced

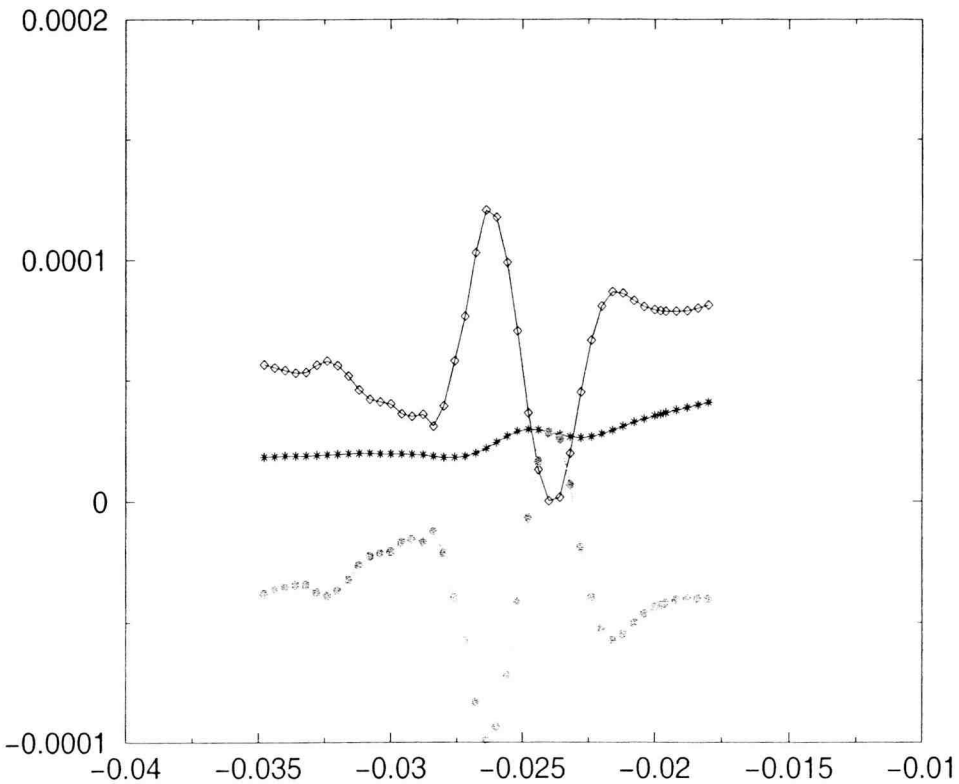

FIGURE 6.3. Change in ΔE for fcc Ni($\lambda_{so} = 100meV$) as a function of one parameter change using Gaussian Fermi surface smearing with $\sigma = 49meV$ and division 60 along a reciprocal lattice vector. The parameter being changed is xyd2_110 spin down. Energy is measured in Rydberg. The diamond is the sum of band 9 and band 10, the filled circle is the sum of band 11 and band 12 obtained from the previous step, and the star is the sum of all those bands and will be used in the next step for each parameter change.

by a certain amount when summed over from the higher bands to the lower bands. Thus, although some bands have a large change in ΔE due to the change in Fermi energy, the total effect actually cancels. The calculations using Gaussian Fermi surface smearing with $\sigma = 49meV$ and division number 60 for two other matrix element changes give the same results. The study of iron showed the same feature.

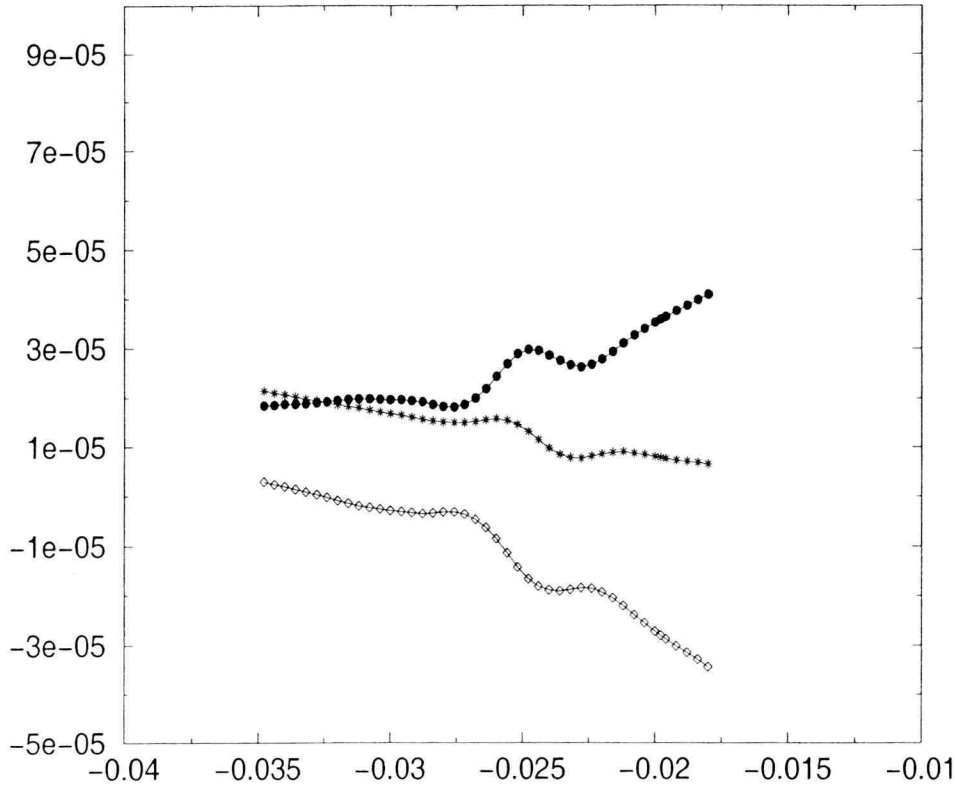

FIGURE 6.4. Change in ΔE for fcc Ni($\lambda_{so} = 100meV$) as a function of one parameter change using Gaussian Fermi surface smearing with $\sigma = 49meV$ and division 60 along a reciprocal lattice vector. The parameter being changed is xyd2_110 spin down. Energy is measured in Rydberg. The diamond is the sum of band 7 and band 8, the filled circle is the sum of band 9 to band 12 obtained from the previous step, and the star is the sum of all those bands and will be used in the next step for each parameter change.

6.3. Correlation with distance to Fermi energy

We next looked at the contribution to the change of energy from each individual star of equivalent k-vectors in the first Brillouin zone. The result is shown in Figure 6.7.

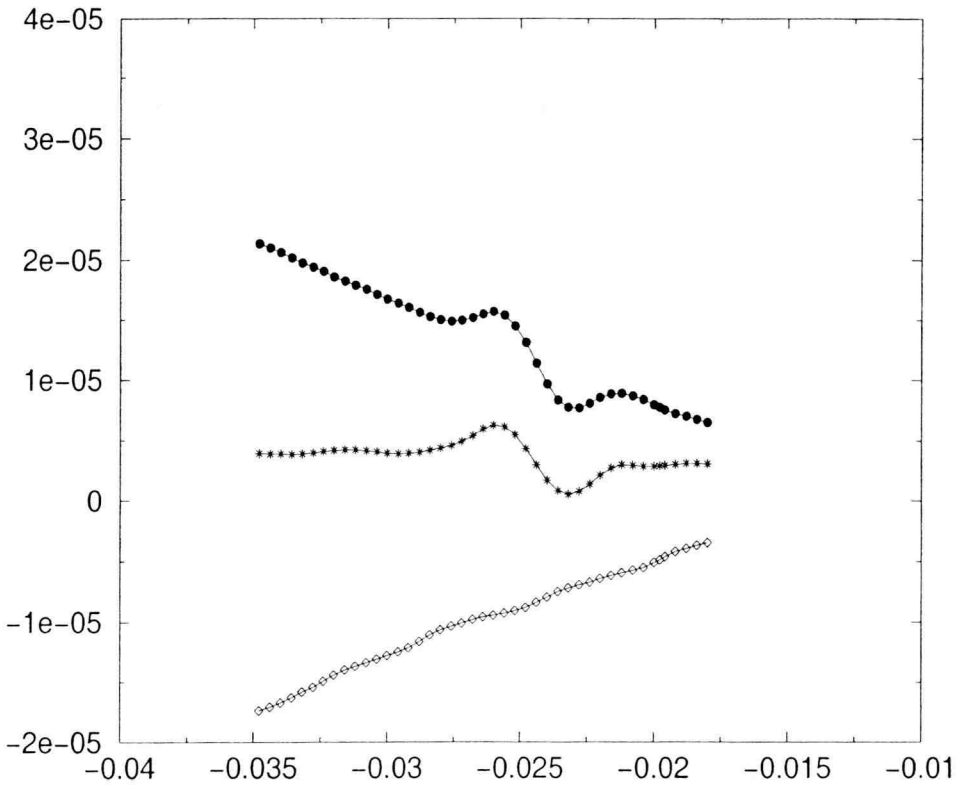

FIGURE 6.5. Change in ΔE for fcc Ni($\lambda_{so} = 100meV$) as a function of one parameter change using Gaussian Fermi surface smearing with $\sigma = 49meV$ and division 60 along a reciprocal lattice vector. The parameter being changed is xyd2_110 spin down. Energy is measured in Rydberg. The diamond is the sum of band 5 and band 6, and the filled circle is the sum of band 7 to band 12 obtained from the previous step, and the star is the sum of all those bands and will be used in the next step for each parameter change.

As we can see from the graphs, stars with a large minimal distance to the Fermi energy do not contribute anything to the change in magnetocrystalline anisotropy energy. Large changes come from the stars that are close to Fermi surface, but not all groups that are close to Fermi surface give rise to a large change in energy. But there is no systematic correlation, and the effects of a large number

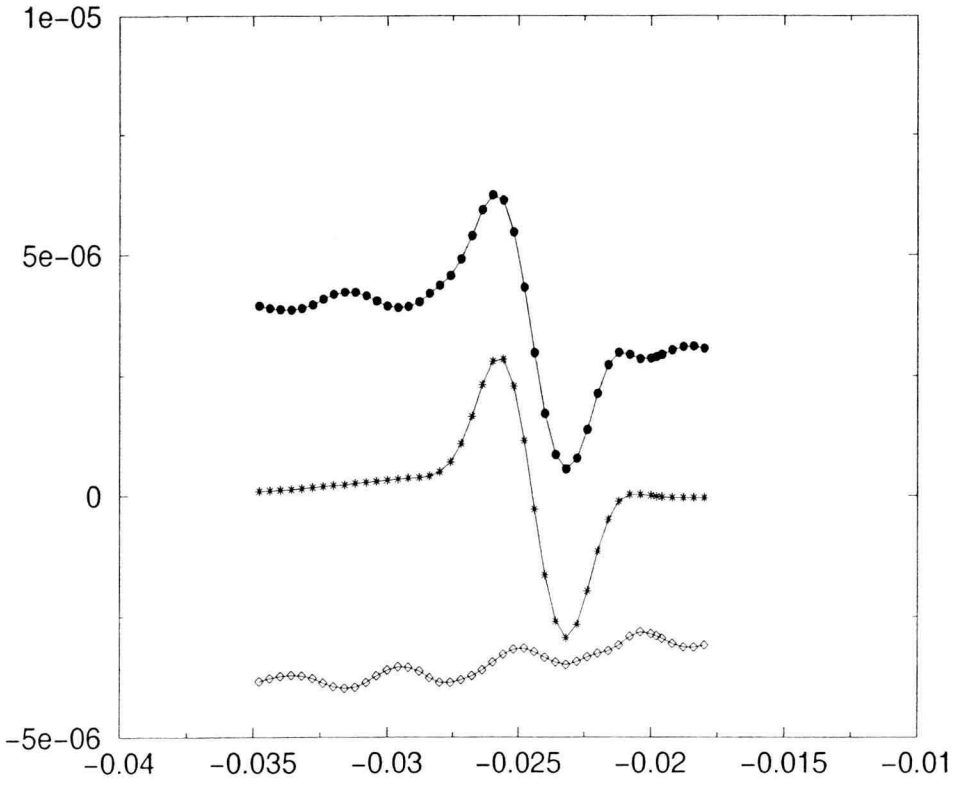

FIGURE 6.6. Change in ΔE for fcc Ni($\lambda_{so} = 100meV$) as a function of one parameter change using Gaussian Fermi surface smearing with $\sigma = 49meV$ and division 60 along a reciprocal lattice vector. The parameter being changed is xyd2_110 spin down. Energy is measured in Rydberg. The diamond is the sum of band 1 to band 4, the filled circle is the sum of band 5 to band 12 obtained from the previous step, and the star gives the final contribution of all the bands to ΔE as a function of parameter change. We did not study the bands numbered from 1 to 4 individually because those bands are totally below the Fermi energy and are fully occupied at all time, thus the contribution of each band is not that significant.

of stars have to be added to get the final answer. All the matrix element changes for both Fe and Ni showed the same behavior.

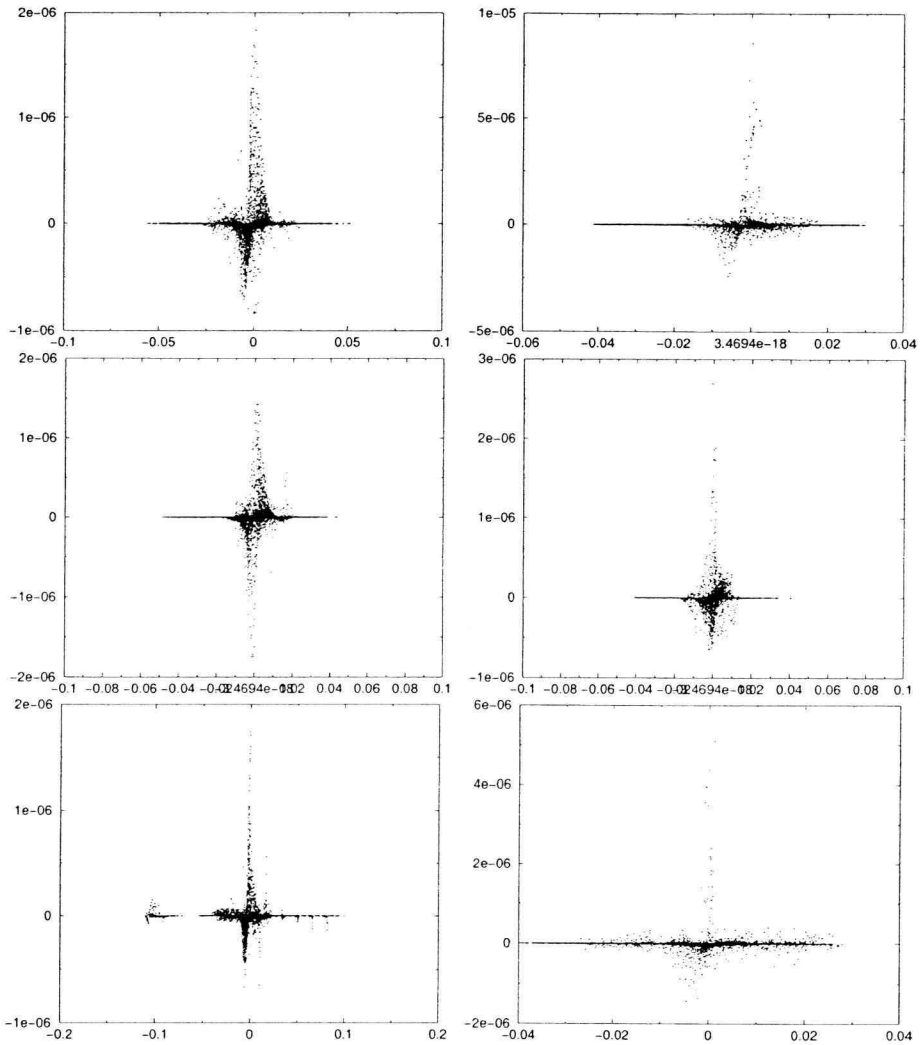

FIGURE 6.7. The change in magnetocrystalline anisotropy energy from each group as a function of the minimum qabsolute distance from the Fermi surface for that group. The left column is for Fe, the right is for Ni. From the top to the bottom, the matrix element being changed for Fe are xyd2_111-up, xyd2_111-down and xyxy_200-up, for Ni, they are xyd2_110-down, xyxy_011-down and xyxy_110-down respectively. The parameter change for each of them is the one that gives the largest absolute change in magnetocrystalline anisotropy energy. Both the change in energy and the distance from the Fermi surface is measured in Rydberg.

6.4. Histograms of the correlation index

For both Ni and Fe we looked at the distribution of the groups in terms of the correlation index, the histograms for both elements for three different parameters are shown in Figure 6.8.

As we can see, the histograms for Fe are distributed, if not evenly, across the whole range, and the histograms show more than one peak in the region. For Ni, on the other hand, the distribution is centered around the value zero and tapers off for larger values of the correlation index.

6.5. Correlation in k-space

We then looked at the stars that have large correlation/anti-correlation with the changes in magnetocrystalline anisotropy energy as a function of parameter change. As shown before, due to the different distribution of the stars, we chose different cut-off values for Ni and Fe. For Fe we just looked at the points whose absolute value of the correlation index is above 0.9, while for Ni we had to lower the value in order to have enough points and we used 0.7 which gave about the same size of sample as for Fe. We only chose those stars that have a relatively large correlation or anti-correlation because we think these should give a systematic description of the observed behavior.

We then located the position of each selected star in the first Brillouin zone and plotted these positions. As shown in the Figure 6.9 and Figure 6.10, for each element the left picture is what we see by looking from $\langle 111 \rangle$, and the right one is from $\langle 001 \rangle$ direction for Ni and $\langle 100 \rangle$ for Fe.

As we can see from the picture for Ni the stars with a large correlation or anticorrelation are all located near the plane $x = y$, and take into account the

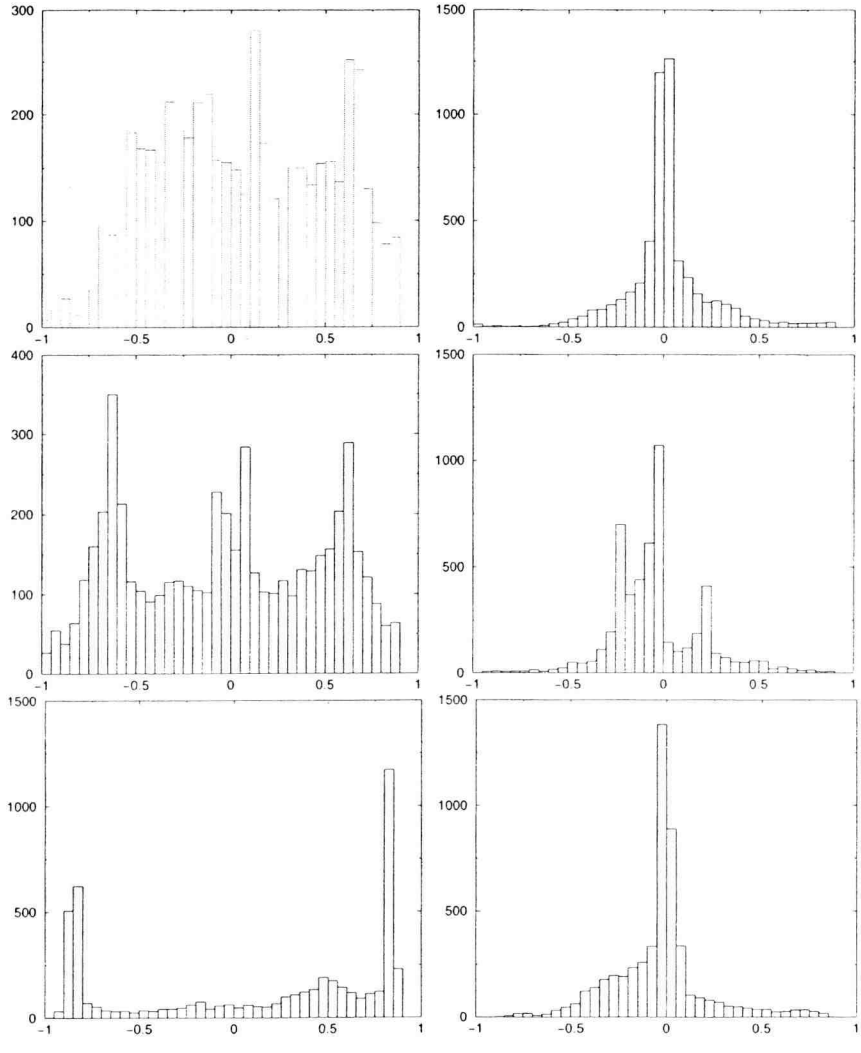

FIGURE 6.8. The change in magnetocrystalline anisotropy energy from each group as a function of the minimum absolute distance from the Fermi surface for that group. The left column is for Fe, the right is for Ni. From the top to the bottom, the matrix element being changed for Fe are xyd2_111-up, xyd2_111-down and xyxy_200-up, for Ni, they are xyd2_110-down, xyxy_011-down and xyxy_110-down respectively. The parameter change for each of them is the one that gives the largest absolute change in magnetocrystalline anisotropy energy. Both the change in energy and the distance from the Fermi surface are measured in Rydberg.

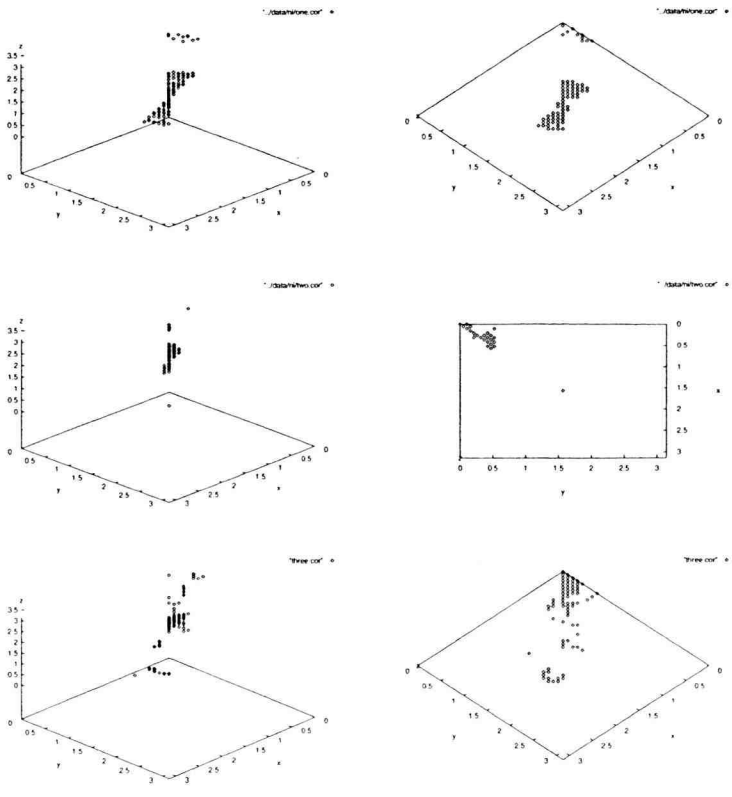

FIGURE 6.9. The stars that are correlated/anti-correlated to the change in energy in the first Brilloun Zone for Ni($\lambda_{so} = 100meV$). The parameter change are xyd2_110-down, xyxy_011-down and xyxy_110-down respectively from the top to the bottom.

fact that we were only looking at one point in each individual group, we can say that the points along or near $\langle 111 \rangle$ give large contribution to the change of magnetocrystalline anisotropy energy. It is possible that among those selected stars some really do not contribute a lot to the change in energy although they are highly correlated or anti-correlated to the overall change in the given range of parameter change. But as we have seen before, that large contribution to magnetocrystalline

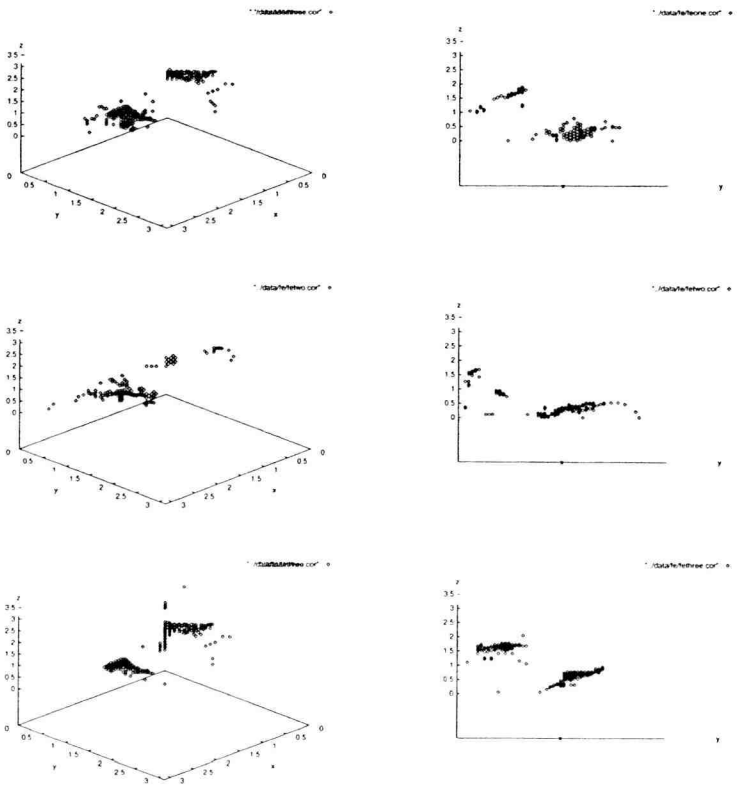

FIGURE 6.10. The stars that are correlated/anti-correlated to the change in energy in the first Brilloun Zone for Fe($\lambda_{so} = 60meV$). The parameter change are xyd2_111-up, xyd2_111-down and xyxy_200-up respectively from the top to the bottom

anisotropy energy is really given by an equivalent group which is close to the Fermi surface, we can safely conclude that for Ni, those groups that are close to Fermi surface and along or near $\langle 111 \rangle$ direction basically decide the overall sensitivity of the magnetocrystalline anisotropy energy on parameter change. We also studied two other parameters which give large change in ΔE, namely xyxy_011

spin down and xyxy_110 spin down both using Gaussian Fermi surface smearing with $\sigma = 49meV$ and division 60 along a reciprocal lattice vector.

In case of Fe we saw something totally different. Changes in all three parameters gave similar results. Those points that have a large correlation/anti-correlation index are mostly crowded around the $z = 0$ plane, and again, taking into account the fact of the symmetry within an equivalent group, those stars that are along $\langle 001 \rangle$ and close to Fermi surface should be the ones that decide the sensitivity as a function of the change in matrix element.

For both Ni and Fe the stars are all along highly symmetric directions, which we believe is reasonable since the effects of spin-orbit coupling are larger because of degeneracies. An interesting result indicated by the calculation is that for Ni it is the points along $\langle 111 \rangle$ direction that give a large contribution while for Fe it is the points along $\langle 100 \rangle$. At this point, it is too early to conclude whether this is decided by the structure of the crystal or not. It could just be a coincidence that the stars that are along the easy axis for both elements decide the sensitivity of the total magnetocrystalline anisotropy energy although the real reason is not known yet. More work should be done on this.

6.6. Correlation with absolute contributions

Finally, we took a look at the relationship between the correlation index and the sum of squares of the contribution to the energy for each individual star. The result are shown in Figure 6.11.

For both Ni and Fe we see no direct relationship between the correlation index and the absolute contribution to the energy. There are large absolute energy contributions for both large and small correlation indexes. The only difference is

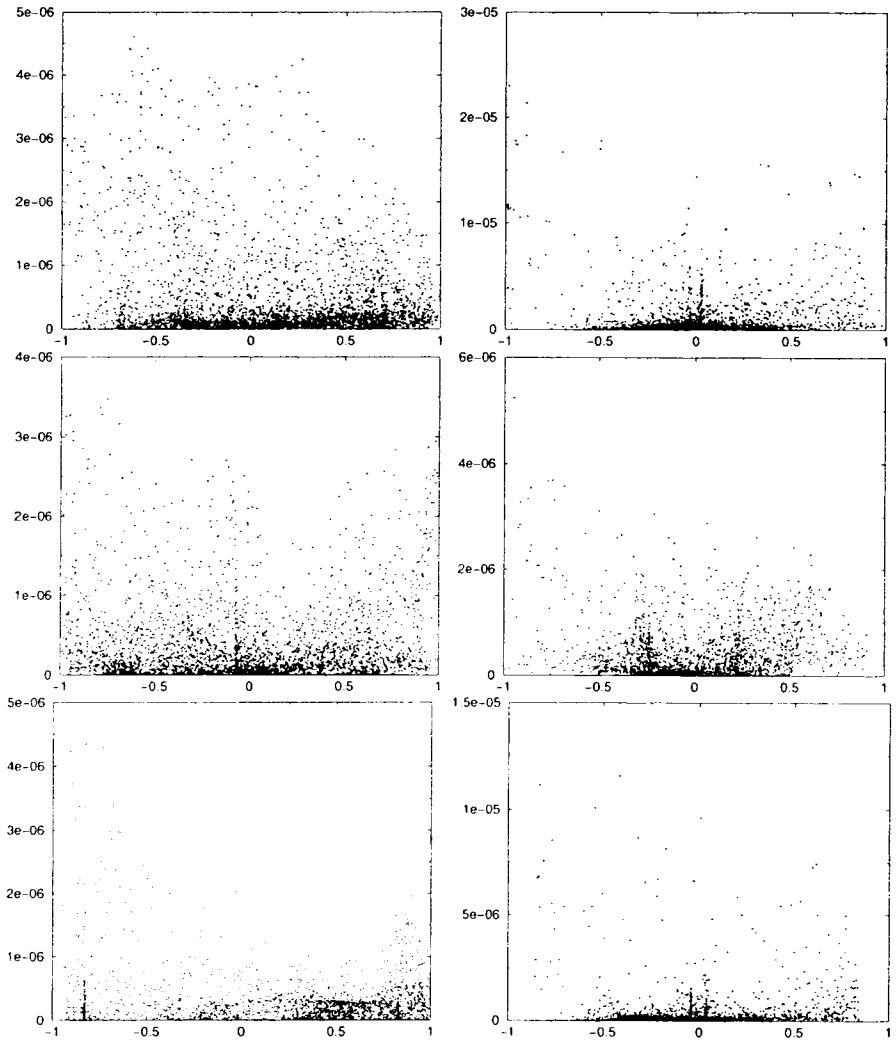

FIGURE 6.11. The total absolute energy change for each equivalent group as a function of the correlation index. The left column is for Fe, the right is for Ni. From the top to the bottom, the matrix elements being changed for Fe are xyd2_111-up, xyd2_111-down and xyxy_200-up; for Ni, they are xyd2_110-down, xyxy_011-down and xyxy_110-down respectively.

that the contribution in energy is relatively larger for Ni than for Fe. It is the same for all the other matrix elements for both Ni and Fe.

6.7. Effect of different smearing parameters

Schneider [1] has already pointed out in his work that for Ni, if one uses broadening larger than the size of spin-orbit coupling strength, the result converges to a wrong value by about 0.07 μeV and suggestes that a larger division and a broadening smaller than the size of spin-orbit coupling strength should be used. What we are observing here is the sensitivity of the magnetocrystalline anisotropy energy with the change in matrix element without requiring the exact value of the energy. Thus using a broadening somewhat larger than the size of the spin-orbit coupling should give a good description of the overall picture although the calculated pattern in the change in magnetocrystalline anisotropy energy might be shifted by a small amount. From the results presented in [1] we see that for our choice of broadening parameter we already capture most of the effects contributing to the energy. In order to check the sensitivity of our results to the choice of broadening we did one parameter change using Gaussian Fermi surface smearing with $\sigma = 96meV$ and division 40, and we observed that the highest two bands also gave the largest contribution to the change in energy, as we summed over from higher bands to the lower bands, the contribution from each individual bands cancels out, and the overall sensitivity of magnetocrystalline anisotropy energy looks pretty much the same with the one using $\sigma = 49mev$ and division 60. Similarly, we found out that the equivalent groups that are close to the Fermi surface give large contribution to the energy change. We also saw that the stars that have a large correlation/anti-correlation are also along $\langle 111 \rangle$ direction. We thus concluded that two broadening parameters really do not make a large difference in describing the overall structure except for a smaller broadening, in order to have the result converge, a larger division should be used as pointed out by Schneider [1].

7. CONCLUSION

A study of sensitivity of the magnetocyrstaline anisotropy energy with respect to changes in the matrix elements of a tightbinding Hamiltonian was carried out for the bcc Fe and fcc Ni.

For both Fe and Ni, we found out that the contribution to the magnetocyrstaline anisotropy energy due to the points near the Fermi surface is in general large compared to those that are far away. But there is a large amount of cancelation of the contribution to the magnetocyrstaline anisotropy energy among these points. As a result, almost all points in the Brillouin zone have to be included in the k-space sums.

When we consider the bands in the crystal, those bands whose energy is comparable to the Fermi energy change most as a function of the change of the matrix element, but neighboring bands cancel out. When summing over all the bands, the biggest change in magnetocyrstaline anisotropy energy is about 100 times smaller than the one we could have for a single band whose energy is about the same with the Fermi energy. Hence we need to add the contributions of all bands.

It is worth mentioning that for Fe, we saw the majority of the k-points whose change in energy changes either in a highly correlated or in a highly anti-correlated manner with respect to the overall change of the magnetocyrstaline anisotropy energy are located along or near $\langle 100 \rangle$ which is the experimental easy axis for Fe. And for Ni, we observed that these points are clustered around $\langle 111 \rangle$ direction, which is the easy axis for fcc Ni. At this point, it is still too early to draw any conclusion about this, but it is highly unlikely just a coincidence, more work should be done on this.

The calculations gave us a huge amount of data, and it is hard to find out a way of analyzing them perfectly taking into account every possible factor. In this work, we just tried to look at this matter in several different ways in order to understand where the important changes in k-space are that contribute a large amount to the changes in the magnetocrystalline anisotropy energy. All of k-space seems to contribute, which points to the conclusion that it is worthwile trying to find a description in real space. Changing parameters in a tightbinding Hamiltonian is a good way to analyze the problem, since these parameters are defined in real space by the overlap of orbitals on neighboring atoms. At some point, however, we need to transform to reciprocal space in order to include the effects of the Fermi surface. It is this dual nature which makes the calculation of the magnetocrystalline anisotropy energy such a hard problem.

BIBLIOGRAPHY

[1] Guenter Schneider. *Calculation of Magneto-crystalline Anisotropy.*

[2] G. H. O. Daalderop, P. J. Kelly, and M. F. H. Schuurmans, Phys. Rev. B **41**, 11919 (1990).

[3] G. Y. Guo, W. M. Temmerman, and H. Ebert, Physica B **172**, 61 (1991).

[4] J. Trygg, B. Johansson, O. Eriksson, and J. M. Wills, Phys. Rev. Lett. **75**, 2871 (1995).

[5] S. S. A. Razee and J. B. Staunton, Phys. Rev. B **56**, 8082 (1997).

[6] S. V. Halilov *et al.*, Phys. Rev. B **57**, 9557 (1998).

[7] S. V. Beiden *et al.*, Phys. Rev. B **57**, 14247 (1998).

[8] A.J. Freeman et al, J. Magn. Magn. Mater. **203**, 1 (1999).

[9] *Landolt-Börnstein, New Series Vol. III/19a*, edited by K. Hellwege and A. M. Hellwege (Springer-Verlag, Berlin, 1987).

[10] Adrian P. Sutton. *Electronic Structure of Materials.* Clarendon Press, 1993

[11] Walter A. Harrison. *Electronic Structure and the Properties of Solids.* Freeman, 1980

[12] Neil W. Ashcroft and N. David Mermin. *Solid State Physics.* Saunders College Publishing, 1976

[13] J. C. Slater and G. F. Koster. *Simplified LCAO Method for the Periodic Potential Problem.* Physics Review, 1954

[14] D. A. Papaconstantopoulos. *Handbook of the Band Structure of Elemental Solids.* Plenum Press, 1986